

Observational Geology of Graphene, at the Nanoscale

Boris I. Yakobson^{†,*} and Feng Ding[‡]

[†]Department of Mechanical Engineering and Materials Science, Department of Chemistry, and the Richard E. Smalley Institute for Nanoscale Science and Technology, Rice University, Houston, Texas 77005, United States, and [‡]Institute of Textiles and Clothing, Hong Kong Polytechnic University, Hong Kong, China

Vista after vista . . . range beyond range.
Thornton Wilder

What one sees and recognizes depends on the scope and the permitted detail of our worlds. Walk around an office, and the world appears comfortably flat and unadventurous. Yet a not-so-distant journey—or simply a binocular—may reveal a mountain ridge or an ocean coast, that is, if you are not in Texas. Embark on an expedition of Magellanian scale, and you may prove the Earth's roundness and perhaps discover continents. Recent advances in microscopy instrumentation reveal both the new, finer atomistic details of a material's makeup and, at the same time, the organization on larger scales. One monoelemental material is of particularly keen and sustained interest.

A monatomic layer of sp^2 -carbon, once obtained by reduction of graphite oxide¹ and called graphene, remained largely overlooked until the physical properties of this material, cleanly peeled off mechanically,² attracted great attention from researchers across a range of fields. Exfoliated this way, pieces are usually small and the atomic structure appears as clean hexagonal tiling, with minor elastic undulations and rather rare point defects—a mono- or divacancy, an interstitial carbon atom, or a Stone–Wales defect 5/7|7/5. Importantly, these defects are not only rare, but they also easily vanish upon annealing: a local transformation and addition or deletion of an atom restores a fully perfect lattice. This contrasts with non-annealable, topological defects. A striking example is a humble lonely pentagon, which imposes a conical shape on the whole lattice around it³ and obviously cannot be eliminated without rearranging an entire macroscopic area. Another example is an extended series of pentagons “5” and heptagons “7”, or rather a series of their

ABSTRACT As the available length ranges expand, graphene begins to show its anticipated polycrystallinity. Its texture, revealed with modern comprehensive microscopy in recent work by Kim *et al.*, includes coherent domains/grains oriented randomly yet with an intriguing degree of regularity. The domains are stitched together by pentagons and heptagons aligned into the grain boundaries. The challenge is now to deduce the mechanisms of formation based on observations and then to find ways to control the morphology toward useful properties and applications.

pairs 5/7. If such series has a balanced polarity (as in 5/7|5/7|7/5/7/5), then it can be annealed locally. If the polarity along the linear series is maintained, it has global consequences and together these 5/7s ensure that the domains/grains separated by such grain boundaries (GBs) are also mismatched in their orientations.

The article by Kim *et al.* in this issue of *ACS Nano* presents a vivid picture of polycrystalline graphene, a careful mapping of the grains/domains reoriented in-plane, tilted with respect to each other at different angles.

The article by Kim *et al.* in this issue of *ACS Nano*,⁴ which is essentially concurrent with a *Nature* paper by Huang *et al.*,⁵ presents a vivid picture of polycrystalline graphene, a first careful mapping of the grains—domains reoriented in-plane, tilted with respect to each other at different angles (Figure 1a).

* Address correspondence to biy@rice.edu.

Published online March 22, 2011
10.1021/nn200832y

© 2011 American Chemical Society

In a *tour de force* of modern microscopy, the studies use complementary methods and careful analysis to yield otherwise unavailable information. While with a greater scope the dark-field imaging and local diffraction techniques enable the researchers to measure the domain misorientations, on a smaller scale, the aberration-corrected high-resolution transmission electron microscopy (HRTEM) further shows the intimate atomistic structure of the seam lines, the borders between the domains. The relative tilt angle varies from 0 to 30°, due to the hexagonal symmetry of real graphene, instead of a 180° range in the schematic depiction of Figure 1a. Data collected from sufficiently large areas show a non-obvious distribution that peaks at smaller and greater tilt angles. To enlarge the sample set, a composite distribution from three sources^{4,5,6} is plotted in Figure 1b,c. In spite of subtle differences in the growth conditions, all samples have been produced on copper foils by chemical vapor deposition (CVD),⁷ which provides good reason for considering such combined statistics. Since the individual reports suggest peaks near certain angles, it is instructive to see what features remain robust across experiments by different groups. Furthermore, one can either directly add the counts (assigning equal weights to each GB found, Figure 1b) or first normalize the data and thus assign the same weight to each report (Figure 1c). Even though the peaks become less conspicuous, a visible dominance of the low angle <7° and especially near 28° GB must be telling us something. This angle distribution is sustained across the experiments, although the different growth conditions do change the size (as large as 3–10 μm in ref 4 or only ~0.2 μm in one growth method of ref 5) and shapes of the grains. Moreover, one notices not only the generic three GBs per node in ref 4 but also often multiple GBs radiating from the apparent growth centers in ref 5. It is

reasonable to speculate that a cleaner substrate and consequently slow homogeneous nucleation would result in larger domains, whereas the presence of centers for heterogeneous nucleation should speed it up, producing smaller grains, likely emanating from the shared hubs. In spite of the apparent grain morphology sensitivity to the growth conditions, the GB angle distribution appears reproducibly non-uniform.

Just months before Kim *et al.*'s⁴ and Huang *et al.*'s⁵ reported observations, three theoretical studies appeared,^{8–10} in which the structures and energies of tilt GBs were systematically compared as a function of the tilt angle. All three viewed the GBs as 5/7 chains, similar of course to the old views of graphite¹¹ and of nanotube junctions,^{12,13} where the change of chirality is equivalent to the tilt angle between the grains. As a natural step from geometry to physics, all groups^{8–10,14} computed the GB energies, shown in the composite plot of Figure 2a. The GB degenerates into a perfect zigzag line at 0° and similarly degenerates into a perfect armchair line at 60°, both with zero energy. As the tilt and the number of 5s and 7s both increase, the energy γ goes up, as well, yet less than in simple proportion to the defect occurrence. For higher 5/7 defect density, there is a mutual cancellation, a “destructive interference” of the stress fields, similar to optics. Indeed, a 5/7 dislocation is not a stress-free void nor a crack, but importantly, it carries a known compression on the 5 side (extra plane-row, blue in Figure 2b,c) and an opposite sign tension on the 7 side (missing plane-row, red in Figure 2b, c). Obviously, these fields are mutually canceled when brought in proximity, thus higher defect density reduces the bond prestrain (which makes the GB seemingly stronger) and the total energy. Consequently, the high-density GB has a slightly lower energy even though it contains more defects. Figure 2c illustrates this with the computed

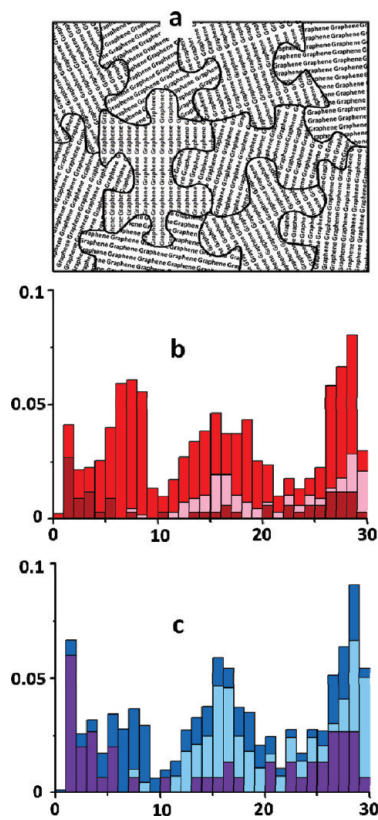


Figure 1. Even in a solidly assembled puzzle, the mismatch in texture orientations creates a pattern of tilt boundaries (a). Composite distributions of the tilt angles from experiments, (b) with equal weight per each grain boundary occurrence, in magenta,⁴ pink,⁵ and red,⁵ or (c) with equal weight per each report, in purple,⁴ light blue,⁶ and blue,⁵ all consistently non-uniform.

continuum stress field (namely, a $\text{Tr } \sigma = \sigma_{xx} + \sigma_{yy}$) around an edge dislocation, visibly greater for a single dislocation (\perp) than for a condensed array in a large angle GB. One could even construct a Heisenberg form of a Hamiltonian, as $H \sim \sum_i |\mathbf{b}_i|^2 - \sum_{ij} J_{ij} \mathbf{b}_i \cdot \mathbf{b}_j$ (note that in the hexagonal lattice the Burgers vector \mathbf{b} accepts six discrete values), and have a basic model of GB handy. Positive “exchange integral” J_{ij} originates from the elastic fields cancellation for the collinear \mathbf{b} s and suggests that such defects want to align and condensate. Direct atomistic calculations do show such an energy dip at 32°, especially pronounced in the accurate density functional theory (DFT) computations.¹⁰ It is tempting to relate this lower

energy with the higher presence of such GB angles in experiments (the equivalent angle would be 28° , within the observed peaks, Figure 1b,c), yet one can find no reason for such an association.

Complementary to the global domain mapping, the intrinsic atomic-scale makeup of the GB lines is of great interest. One thing is to propose a logical bond topology of GB¹¹ or to compute its precise geometries through energy minimization,^{8–10,14} yet another thing is to see it—and believe it. This is what high-resolution microscopy offers to an inquisitive observer.⁴ HRTEM reveals only 5s and 7s, predominantly next to each other—that is, the disclinations paired up into dislocations of smallest Burgers vectors ($\pm 1,0$), and with neither vacancies nor interstitials. This suggests good local equilibration at growth conditions: any low-energy void site is filled with a carbon atom, every high-energy interstitial C is expelled, and every unnecessary Stone–Wales defect is switched off. Even though it remains unclear how statistically representative an image or two might be, the reported pattern⁴ is quite remarkable, especially in its striking visual similarity with the related pattern, obtained completely independently.⁵ One is left to wonder to what extent this is indeed a most typical GB structure, or a coincidental similarity. While resolving the planar atomic positions, the HRTEM may conceal the three-dimensional landscape, and theoretical calculations can help restoring it. To this end, one can extract all atomic x – y positions and then perform full energy minimization in x – y – z space, as in ref 8. The resulting structure in Figure 3 shows significant off-plane warping. (It is possible then that the visibly “distorted” hexagons in the ADF-STEM image⁵ are simply not parallel to the plane of view.) This warping of a free-suspended GB area is of course suppressed if the structure is laid on a substrate, with accordingly changed energies. The meandering

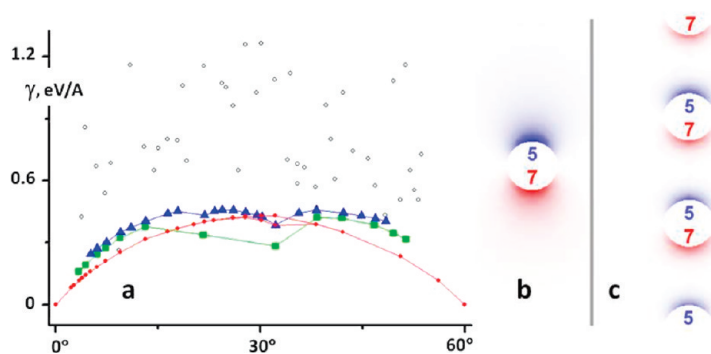


Figure 2. Grain boundary energy varies with the tilt angle and is sensitive to the local organization of the 5 and 7 pairs. (a) Data shown from different computations: hollow circles⁹ (TBA), blue triangles¹⁴ (classical force field), red circles (AIREBO potential as in ref 8), and green squares¹⁰ (DFT). (b) Computed continuum stress field from an isolated edge dislocation, and (c) from a series in the grain boundaries, with apparent mutual cancellation, explaining a dip in energy near $\sim 30^\circ$; blue is for compression and red is for tension.

of GB is another striking feature that may or may not be typical. Both this meandering and the aperiodic positions of the 5/7s imply that the GB is unlikely the lowest energy structure for a given tilt angle.

Energy is an omnipotent and loved measure in physics, and its minimization guides various processes, in particular, the structural stability or the fluctuations off equilibrium, whose probabilities correlate with $\sim \exp(-E/k_bT)$. However, both dislocations and GB are non-thermodynamic objects; they do not emerge as results of fluctuations but are kinetically “frozen” and do not need to obey the laws of statistical physics in this sense. In this respect, a GB is similar to a mountain ridge—a strikingly improbable object from the energy minimization viewpoint, yet not uncommon. To try to understand the GB morphology and the tilt angle distributions one should track back along their past origin pathways and not simply compare their present energies. Similarly, a geologist is forced to do retro-engineering because the objects of his study were shaped by slow processes long ago. When the continental activity almost seized in Precambrian times or the Paleocene, there was not a soul there to watch and to record what was going on and how. The geologist does his fieldwork now, observes what is available, and tries to deduce how it came about. For the nanostructures,

the formation processes may be too fast for an *in situ* record, so we resort to a similar approach: record the final state morphology and then guess what factors could have caused its formation. “Observational geology” of graphene, made possible by the advances in microscopy, suggests that its monocrystalline domains and the GBs between them must originate during growth and the tilt angle distribution may be determined by the degree of epitaxy to the substrate at the earliest stages of nucleation.

A grain boundary is similar to a mountain ridge—a strikingly improbable object from the energy minimization viewpoint, yet not uncommon.

The possibility that the GBs are “induced” by the underlying texture of polycrystalline Cu is ruled out since the size of graphene domains is at least an order of magnitude

smaller than the granularity of copper foils in use.^{4,5} If graphene growth was not epitaxial at all, one would expect random grain orientations and a uniform distribution of the GB tilt. On the other hand, strong epitaxial match to a monocrystal substrate would permit only very few GB angles and sharp peaks in the tilt distribution for the CVD produced graphene. Small sp^2 -nuclei of graphene are likely to start near the substrate steps¹⁵ and are also likely to have preferred orientations, not necessarily the same as for an extended graphene sheet. As the nucleus island grows, its mobility on a substrate rapidly decreases and soon it adapts an orientation that remains frozen, unchanged afterward. Investigations of the lowest energy clusters can be rather tedious¹⁵ but offer a possible way to understand GB tilts. For example, while a *coronene*-like cluster has its lattice properly packed with hexagons embracing the metal atoms (Figure 4a), interestingly, a larger cluster of *circumcoronene* type C_{54} , according to one calculation,¹⁶ is tilted at an angle of $\sim 14^\circ$. If an island preserves this orientation and eventually encounters another grain frozen in a mirror-twin position as in Figure 4b, the emerging grain boundary has a tilt of (bingo!) $\sim 28^\circ$. The emerging contact boundary is illustrated in Figure 4c. Although this may well be a coincidence, the possibility of graphene domains being trapped in the local minima at earlier stages in their formation is a probable cause for the complexity of the grain orientations. More frequent grain orientations may correspond to their epitaxial match to Cu(111) at early stages of nucleation and small island growth. If nucleation is favored near the steps on a metal surface, as both calculations¹⁵ and some experiments¹⁷ suggest, then the orientations of such steps and terraces can play a definitive role in the morphology of finished graphene “quilts” (Figure 5). Who knew that the dull-gray material graphite, when seen

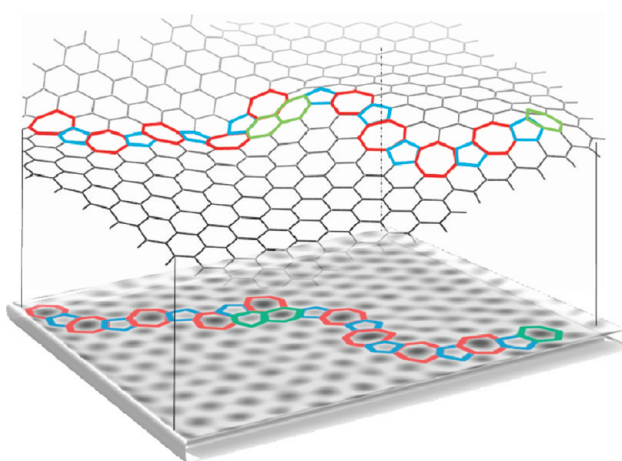


Figure 3. Pentagons (blue) and heptagons (red) in a grain boundary should result in noticeable off-plane 3D landscapes,⁸ obtained here by computational relaxation, for an example based on aberration-corrected annular dark-field scanning transmission electron microscopy (ADF-STEM) image,⁵ bottom. Bottom part adapted with permission from ref 5. Copyright 2011 Nature Publishing Group.

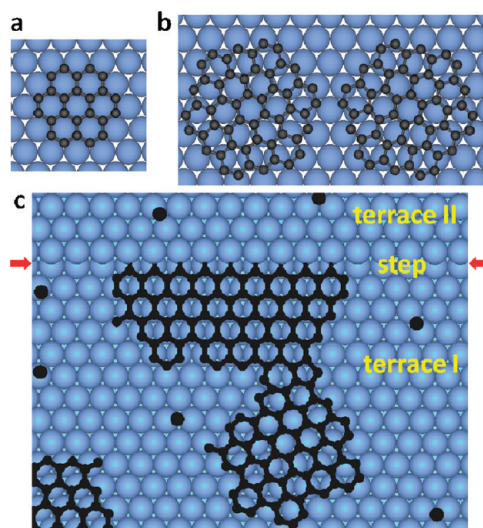


Figure 4. “Multi-epitaxial” growth process may result from different ground state orientations relative to the metal substrate, when a smaller cluster (a) is then rotated by *ca.* 14° . If trapped in these orientations (b), two such islands can form a high-angle boundary. Preferential nucleation at a step¹⁵ can further determine a subset of specific tilts, which requires further detailed study.

through the rigorous technological eyes of modern microscopy, would turn into such a post-impressionist play of color and form? Yet here it is, the colored map of the *united domains of graphene*, inviting and unexplored in many corners.

PRACTICAL CONSEQUENCES AND LOOKING TO THE FUTURE

What are the practical consequences beyond the fascinating patterns, maps, and colored quilts revealed by microscopy? Generally,

polycrystals can outperform monocrystals, sometimes impressively. In magnetic materials, GBs suppress the Bloch walls mobility and help to tune material hardness (magnetic coercivity); this seems irrelevant to generally nonmagnetic graphenes, except for the ferromagnetism of the defects themselves. In mechanics, well-known grain boundary strengthening culminates in the Hall–Petch relationship, where the smaller domains suppress the dislocation mobility, so the yield



Figure 5. A 25 μm view, with color-coded orientations of graphene domains, each smaller than the copper grains, yet some visibly grown across the copper grain boundaries, marked out by white lines. (Courtesy of P. Huang and D. A. Muller, Cornell University.)

stress increases inversely to the domain size, $\Delta\sigma_{\text{yield}} \sim 1/\sqrt{d}$. Graphene, however, is nonductile; its 5/7 dislocations are sessile at practical temperatures.¹¹ Grain boundaries work as stress concentrators for easier brittle failure, as recent experimental tests show, as well.⁵ Electrical resistance does not appear to be significantly increased by the apparently irregular grain boundaries,⁵ while theoretical analysis suggests that for the charge carriers almost complete transparency or reflection can both be expected from the periodic arrays of dislocations.¹⁸ On the basis of recent observations and the basic fact that the GB structure is not well equilibrated but is rather frozen in disorder, it may be challenging to engineer a periodic array accurately. An interesting exception is a special case of non-tilt GB, a translational variety where strong order in a defect sequence

$$\begin{array}{c} 5 & 5 & 5 & 5 \\ 8 & - & 8 & - & 8 & - & 8 \\ 5 & 5 & 5 & 5 \end{array}$$

is well-maintained by its rigid attachment to the zigzag rows in the native lattice, whose halves are stacked slightly off (hcp and fcc) on the Ni(111) surface.¹⁹

Beyond the captivating patterns unearthed by “nano-geology” field work, there lie various tantalizing possibilities. There is a striking difference between geology and nanoscience: In the former, one can figure out the origin of the observed structures but cannot repeat the experiment and cannot direct its conditions toward a desired outcome. In a nanotechnology lab, this is possible. The emerging understanding relates the specific scales with the periods of nanoformations. Locally, in the smallest atomistic scale (~ 0.5 nm), the GBs appear well equilibrated and at the lowest available energy, that is why one sees no unnecessary disorder, but only inevitable 5/7s (or 4|8s in the shear type GB). On a somewhat larger scale (~ 1 –10 nm), the 5/7s become unruly and the GB lines meander, with the lowest energy no longer being a reliable foothold. One can speculate that these shapes are frozen, inherited from the instabilities of the growing fronts of individual domains. Indeed, the front of growing graphene either can remain straight (probably zigzag, as a slowest-growing facet²⁰) or at certain conditions can develop undula-

tions through the known Mullins–Sekerka instability in diffusion-controlled aggregation. At this intermediate time, shapes at the front may freeze as a tortuous GB when the two fronts finally meet and close the gap. This can possibly be avoided by changing growth conditions. On the even larger scales of the entire domains (50–1000 nm), their orientations can in fact be established even earlier, at the beginning nucleation stage. A set of selected low-energy small islands can ultimately develop into the non-uniform distribution of the tilt GB in the complete polycrystal. Better understanding each stage of growth can enable morphological control at the corresponding length scales and ultimately allow us to engineer the networks of built-in one-dimensional nanostructures with desired mechanical, chemical, magnetic, and electronic (both longitudinal and transverse) properties.

Acknowledgment. Work at Rice was supported by the Office of Naval Research, the Robert Welch Foundation, and the National Science Foundation. We are grateful to Y. Liu, V. I. Artyukhov, and M. Liu for help and useful discussions.

REFERENCES AND NOTES

- Boehm, V. H. P.; Clauss, A.; Fischer, G. O.; Hofmann, U. Z. Dünne Kohlenstoff-Folien [Thinnest Carbon Films]. *Naturforsch.* **1962**, *17b*, 150–153.
- Novoselov, K. S.; Geim, A. K.; Morozov, S. V.; Jiang, D.; Zhang, Y.; Dubonos, S. V.; Grigorieva, I. V.; Firsov, A. A. Electric Field Effect in Atomically Thin Carbon Films. *Science* **2004**, *306*, 666–669.
- Krishnan, A.; Dujardin, E.; Treacy, M. M. J.; Hugdahl, J.; Lynum, S.; Ebbesen, T. W. Graphitic Cones and the Nucleation of Curved Carbon Surfaces. *Nature* **1997**, *388*, 451–454.
- Kim, K.; Lee, Z.; Regan, W.; Kisielowski, C.; Crommie, M. F.; Zettl, A. Grain Boundary Mapping in Polycrystalline Graphene. *ACS Nano* **2011**, *10*.1021/nn1033423.
- Huang, P. Y.; Ruiz-Vargas, C. S.; van der Zande, A. M.; Whitney, W. S.; Levendorf, M. P.; Kevek, J. W.; Garg, S.; Alden, J. S.; Hustedt, C. J.; Zhu, Y., *et al.* Grains and Grain Boundaries in Single-Layer Graphene Atomic Patchwork Quilts. *Nature* **2011**, *469*, 389–392.
- An, J.; Voelkl, E.; Suk, J.; Li, X.; Magnuson, C. W.; Fu, L.; Tiemeijer,

- P.; Bischoff, M.; Freitag, B.; Popova, E.; *et al.* Domain (Grain) Boundaries and Evidence of Twin Like Structures in CVD Grown Graphene. 2010, arXiv: 1010.3905v1.
7. Li, X.; Cai, W.; An, J.; Kim, S.; Nah, J.; Yang, D.; Piner, R.; Velamakanni, A.; Jung, I.; Tutuc, E.; *et al.* Large-Area Synthesis of High-Quality and Uniform Graphene Films on Copper Foils. *Science* **2009**, *324*, 1312–1314.
 8. Liu, Y.; Yakobson, B. I. Cones, Pringles, and Grain Boundary Landscapes in Graphene Topology. *Nano Lett.* **2010**, *10*, 2178–2183.
 9. Malola, S.; Häkkinen, H.; Koskinen, P. Structural, Chemical, and Dynamical Trends in Graphene Grain Boundaries. *Phys. Rev. B* **2010**, *81*, 165447.
 10. Yazyev, O. V.; Louie, S. G. Topological Defects in Graphene: Dislocations and Grain Boundaries. *Phys. Rev. B* **2010**, *81*, 195420.
 11. Thomas, J. M.; Roscoe, C. Nonbasal Dislocations in Graphite. In *Chemistry and Physics of Graphite*; Walker, P. L., Ed.; Marcel Dekker: New York, 1968; Vol. 3, pp 1–44.
 12. Chico, L.; Crespi, V. H.; Benedict, L. X.; Louie, S. G.; Cohen, M. L. Pure-Carbon Nanoscale Devices: Nanotube Heterojunctions. *Phys. Rev. Lett.* **1996**, *76*, 971–974.
 13. Yakobson, B. I. Mechanical Relaxation and “Intramolecular Plasticity” in Carbon Nanotubes. *Appl. Phys. Lett.* **1998**, *72*, 918–920.
 14. Liu, T.-H.; Gajewski, G.; Pao, C.-W.; Chang, C.-C. Structure, Energy, and Structural Transformations of Graphene Grain Boundaries from Atomistic Simulations. *Carbon* **2011**, *49*, 1016–1031. doi:10.1016/j.carbon.2011.01.063.
 15. Gao, J.; Yip, J.; Zhao, J.; Yakobson, B. I.; Ding, F. Graphene Nucleation on Transition Metal Surface: Structure Transformation and Role of the Metal Step Edge. *J. Am. Chem. Soc.* **2011**, *133*, 1021–1027. doi:10.1021/ja110927p.
 16. Zhang, W.; Wu, P.; Li, Z.; Yang, J. First-Principles Thermodynamics of Graphene Growth on Cu Surface. 2011, arxiv.org/abs/1101.3851.
 17. Sutter, P. W.; Flege, J.-I.; Sutter, E. A. Epitaxial Graphene on Ruthenium. *Nat. Mater.* **2008**, *7*, 406–411.
 18. Yazyev, O. V.; Louie, S. G. Electronic Transport in Polycrystalline Graphene. *Nat. Mater.* **2010**, *9*, 806–809.
 19. Lahiri, J.; Lin, Y.; Bozkurt, P.; Oleynik, I. I.; Batzill, M. An Extended Defect in Graphene as a Metallic Wire. *Nat. Nanotechnol.* **2010**, *5*, 326–329.
 20. Ding, F.; Harutyunyan, A. R.; Yakobson, B. I. Dislocation Theory of Chirality-Controlled Nanotube Growth. *Proc. Natl. Acad. Sci. U.S.A.* **2009**, *106*, 2506–2509.